Simultaneous imaging of multiple focal planes using a two-photon scanning microscope

W. Amir,[1] R. Carriles,[2] E. E. Hoover, T. A. Planchon, C. G. Durfee, and J. A. Squier

Department of Physics, Colorado School of Mines, Golden, Colorado 80401, USA
[1]*wamir@miones.edu*
[2]*rcarrile@mines.edu*

Received March 15, 2007; accepted April 1, 2007;
posted April 20, 2007 (Doc. ID 81110); published June 6, 2007

Despite all the advances in nonlinear microscopy, all existing instruments are constrained to obtain images of one focal plane at a time. In this Letter we demonstrate a two-photon absorption fluorescence scanning microscope capable of imaging two focal planes simultaneously. This is accomplished by temporally demultiplexing the signal coming from two focal volumes at different sample depths. The scheme can be extended to three or more focal planes. © 2007 Optical Society of America

OCIS codes: 180.5810, 180.6900, 110.0180.

Optical microscopy is a well-established tool for scientific and technological research. Its impact continues to grow driven by new developments in detectors, excitation sources, data processing, optical systems, chemical labels, scanning techniques, etc. Confocal and nonlinear techniques such as second-harmonic generation (SHG), third-harmonic generation (THG), and two-photon absorption (TPA) allow three-dimensional (3D) imaging through optical sectioning [1–3]. However, despite all the advances in the field, to our knowledge all commercial nonlinear optical microscopes are restricted to image only one focal plane at a time. The standard method to partially overcome this restriction is to acquire images from different focal planes in rapid succession by scanning the sample in the z direction using piezoelectric translators. However, this approach is not fast enough to follow some intracellular transport and dynamical processes. To the best of our knowledge, the only scheme that has been proposed for simultaneous image acquisition from two different depths is that of Prabhat and co-workers [4]. Their technique is based on modifying the detection pathway of a conventional linear fluorescence microscope to relay images from different sample depths into two separate CCD cameras. Since the scheme is based on linear fluorescence, it suffers from lack of sectioning capability and bleaching problems.

In this Letter we propose a novel technique called simultaneous multidepth acquisition for real-time imaging (SMARTI) that allows simultaneous acquisition of images from two or more focal planes. We demonstrate the scheme for the case of two image planes, but it can be extended to three or more. The excitation pathway of a standard homebuilt TPA scanning microscope was modified to produce a beam consisting of two interlaced pulse trains with different divergence properties. After the objective the two trains will focus at different depths into the sample. Since the fluorescence signal photons are emitted a few nanoseconds after the exciting fundamental pulse, the use of a fast switch that toggles between two channels at the modified repetition rate allows the separation of the two depths. The detection arm of the microscope consists of a photomultiplier tube (PMT), a temporal demultiplexer to separate the signal from each depth, and two fast counters (one for each depth).

The microscope setup is shown in the main panel of Fig. 1. A Ti:sapphire laser beam with repetition rate of 23 MHz (period $\tau \approx 43$ ns), 210 mW average power, 800 nm central wavelength, and 70 fs pulse duration is divided into two arms by a polarizing cube beam splitter. A half-wave plate located before the beam

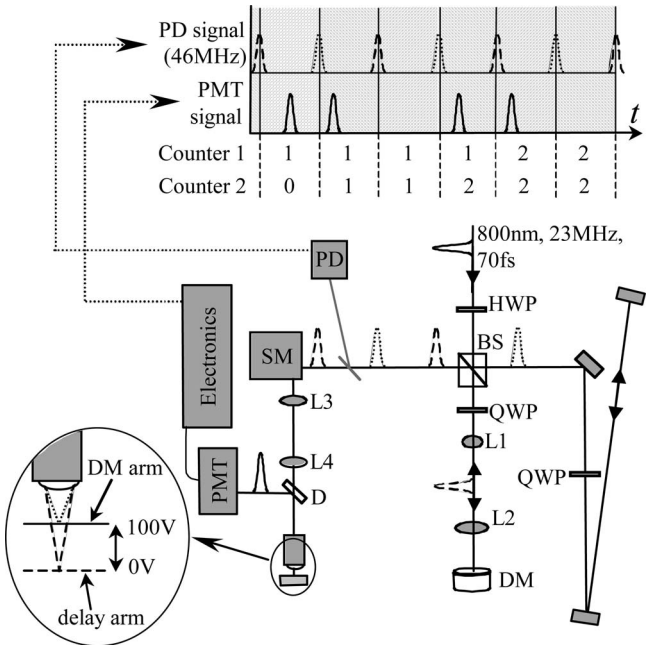

Fig. 1. SMARTI setup: HWP, half-wave plate; BS, polarizing cube beam splitter; QWP, quarter-wave plate; L_1–L_4, lenses ($L_1 = 100$ mm, $L_2 = 200$ mm, $L_3 = L_4 = 100$ mm); DM, deformable mirror; PD, photodiode; SM, scanning mirrors; D, dichroic mirror; PMT, photomultiplier tube. Dotted (dashed) line pulses represent pulses coming from the delay (DM) arm. Top inset, relative timing of the master clock and PMT signal. Pulses from the master clock (PD signal) have a well-defined period, while PMT signal pulses can shift in time due to fluorescence lifetime; counters 1 and 2 represent how the values stored in each counter change with time.

splitter controls the power ratio between the two arms; it is adjusted to have the same power from both arms after the objective. One part of the beam is retroreflected by a 25-mm-diameter, 37-actuator-membrane Agiloptics deformable mirror (DM). The beam divergence is controlled by the variable curvature of the mirror. In order to keep the beam size constant at the entrance pupil of the objective, the DM surface is imaged to this aperture. This is accomplished in two steps: first, a telescope (lenses L_1 and L_2) images the DM surface to the middle plane between the scan mirrors, and then this plane is imaged by another telescope (lenses L_3 and L_4) onto the objective entrance pupil, as required by scanning microscopy. The other part of the original beam is delayed by half its period (≈21.5 ns) with respect to the pulses from the DM arm. Both arms include quarter-wave plates that, when double passed, change the polarization of the beams, thus allowing their recombination at the beam splitter from where the beam is sent to a conventional multiphoton scanning microscope.

After recombination the beam consists of a 46 MHz pulse train. It is focused using a 0.65 NA objective (40×, Zeiss A-plan). As mentioned before, the pulses coming from the DM arm focus at a different depth than those from the delay arm. A PMT (Hamamatsu H7422P-40) is used to collect the backscattered two-photon absorption fluorescence signal after the dichroic mirror, and a BG39 colored glass filter is used to block the residual fundamental beam. The PMT pulses are sent through a 1 GHz amplifier and timing discriminator (Ortec 9327) that produces nuclear instrumentation module (NIM) pulses and then through a NIM to transistor–transistor logic (TTL) translator (Philips Scientific 726). A small part of the fundamental beam is picked up before the scanners, sent to a photodiode, and converted to TTL; this signal represents the 46 MHz pulse train used as the master clock. A field programmable gate array card (Altera DE2) has been programmed to act as demultiplexer, switching the incoming PMT signal between two channels with every pulse of the master clock. These two channels go to fast counters, also programmed into the card, that count the signal from different depths. The separation of the pulses is possible because the fluorescence lifetime is shorter than the fundamental beam pulse separation (see top inset in Fig. 1). If the switching is done at the master clock repetition rate, then a photon occurring between pulses will come from a specific depth.

We calibrated the displacement of the DM arm focal plane with respect to the delay arm focal plane as a function of the DM applied voltage for two different microscope objectives: 40× Zeiss water immersion IR-Achroplan 0.8 NA and 40× Zeiss A-plan 0.65 NA. The results are shown in Fig. 2. For the first objective we measured the relative displacement using two different telescopes in the DM arm. The circles show the results using a 1:4 telescope (where lens L_2 = 200 mm was replaced by a 400 mm lens and the DM position adjusted accordingly); the maximum focal plane displacement is approximately 110 μm. The

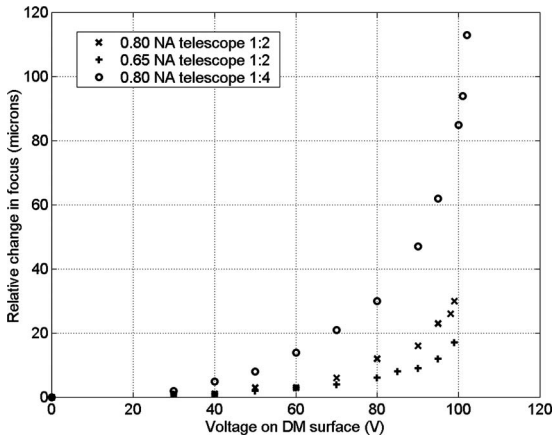

Fig. 2. Displacement of the DM focal plane, with respect to the delay arm, as a function of voltage applied to the DM for two different objectives (40× Zeiss A-plan 0.65 NA and 40× Zeiss water immersion IR-Achroplan 0.8 NA). Different telescope magnifications of 1:2 ("×" marks) and 1:4 (circles) were used for the 0.8 NA objective, showing the influence of magnification on achievable depth. The results for the 0.65 NA objective, using the 1:2 telescope, are shown by the "+" marks. Voltage is applied to all the DM actuators to provide only the focus term.

"×" marks are the results from the same objective using the 1:2 telescope, but in this case the maximum displacement is 30 μm; although this telescope provides less relative displacement, we end up using it for our measurements due to clipping problems when using the other telescope. The results for the second objective are shown by "+" marks on Fig. 2, the maximum displacement with respect to the delay arm is 20 μm. The aberrations from these objectives have been characterized using 2D spectral interferometry [5]. The DM can also be used to compensate for spherical aberration [6–8].

To demonstrate the technique we applied a voltage to the DM to give a depth difference of approximately 9 μm between the focal volumes of both arms; we then took images of 15 μm carboxyl microspheres mixed with Lucifer yellow dye and suspended them in agarose. Figure 3(a) shows a white-light microphotograph of the scanned region containing three microspheres. First, we physically blocked one arm at a time and used a conventional data acquisition card (National Instruments PCI-6111) to record TPA fluorescence images from both depths independently. The results appear on Figs. 3(b) and 3(c), the left (right) panel was taken by blocking the delay (DM) arm. It is clear that each image is looking at a different depth, one at a plane intersecting the top of the three microspheres, and the other intersecting their equators. We then unblocked both arms and used the programmable card to scan the same area of the sample, thus taking TPA fluorescence images of both planes simultaneously; the results are shown in Figs. 3(d) and 3(e). These images agree very well with the ones taken by blocking each arm individually. It is worth noting the reduction in background noise in the SMARTI images (based on photon counting) as compared with the conventional imaging scheme.

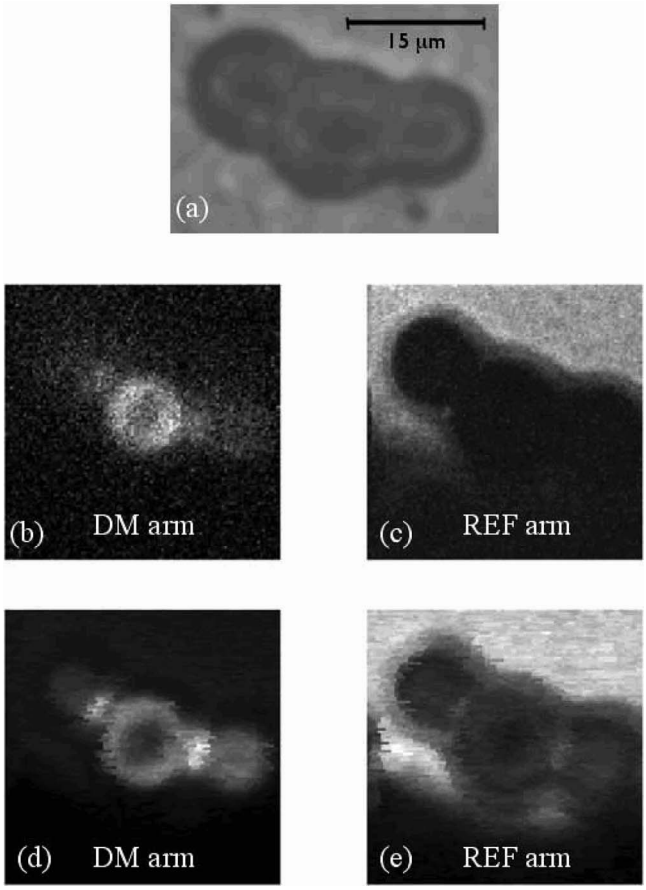

Fig. 3. Images of 15 μm microspheres on Lucifer yellow dye and suspended in agarose: (a) white-light microphotograph of the scanned area, (b) and (c) TPA fluorescence images obtained by blocking the delay (DM) arm of the microscope and using conventional acquisition scheme, (d) and (e) TPA fluorescence images obtained simultaneously using the SMARTI technique. All TPA images are 101×101 pixels REF, images from the delayed arm.

The images shown in Fig. 3 were all taken with the Zeiss A-plan 0.65 NA objective. The first node of the axial distribution of the point-spread function for an infinity conjugate source at 800 nm for such objective is expected to be 3.8 μm. Since the DM arm is not infinite conjugate, its axial resolution is expected to degrade. We used a thin layer of Rhodamine 6G in water to take z scans of both arms to characterize their axial resolution by taking the derivative of the measured z scan profile. For the delayed arm we obtained a derivative with a full width at half-maximum of 3.5 μm, while for the DM arm the value grew to 4.6 μm due to the divergence of the beam.

The technique can be easily extended to more than two simultaneous depths by using multiple arms with different divergences and increasing the number of demultiplexer channels and counters. The maximum number of resolvable channels will be given by the ratio between the repetition period of the laser and the fluorescence lifetime of the signal. If instead of TPA we were to use an instantaneous process such as SHG or THG, the ultimate limit to the number of channels would be given by the acquisition electronics speed.

In conclusion, we demonstrate a two-photon absorption scanning microscope capable of imaging two focal planes simultaneously. This is accomplished with temporal demultiplexing of the signal coming from two focal volumes at different sample depths. The technique can be extended to more than two depths. We believe this technique to be able to improve the 3D image capabilities of future nonlinear microscopes.

The authors acknowledge Tor Vestad for providing the samples. This work was partially supported by the National Institute of Biomedical Imaging and Bioengineering under BRPEB003832.

References

1. W. Denk, J. H. Strickler, and W. W. Webb, Science **248**, 73 (1990).
2. G. J. Brakenhoff and K. Visscher, in *Handbook of Biological Confocal Microscopy*, J. B. Pawley, ed. (Plenum, 1995), p. 355.
3. J. Squier and M. Müller, Appl. Opt. **38**, 5789 (1999).
4. P. Prabhat, S. Ram, E. S. Ward, and R. J. Ober, IEEE Trans. Nanobiosci. **3**, 237 (2004).
5. W. Amir, T. A. Planchon, C. G. Durfee, J. A. Squier, P. Gabolde, R. Trebino, and M. Müller, Opt. Lett. **31**, 2927 (2006).
6. M. A. A. Neil, R. Juskaitis, M. J. Booth, T. Wilson, T. Tanaka, and S. Kawata, J. Microsc. **200**, 105 (2000).
7. L. Sherman, J. Y. Ye, O. Albert, and T. B. Norris, J. Microsc. **206**, 65 (2002).
8. P. N. Marsh, D. Burns, and J. M. Girkin, Opt. Express **11**, 1123 (2003).